Journal of Research of the National Bureau of Standards Vol. 62, No. 6, June 1959 Research Paper 2958

Pits in Metals Caused by Collision With Liquid Drops and Soft Metal Spheres

Olive G. Engel

An equation is developed to give pit depth as a function of collision velocity for pits formed in soft to medium-hard metal plates as a result of collision with liquid drops. The rear face of the target plate must be a free surface. The plate thickness must not be less than 1.5 to 2.0 times the drop diameter nor greater than 4 to 5 times the drop diameter. It is shown that, under the same conditions on the target plate, the equation is also applicable to pits formed in soft to medium hard metal plates as a result of collision with spheres of the same metal that flow radially as a result of the collision. Pit-depth-versus-velocity data obtained in other laboratories were used to test the equation. Metals used as targets were copper, 1100–0 aluminum, 2024–0 aluminum, lead, steel, soft iron, and zinc. Mercury was used as the drop liquid against copper, aluminum, lead, and steel. Water was used as the drop liquid against copper, aluminum, and lead. Spheres of copper, aluminum, lead, soft iron, and zinc were used against targets of the same materials, respectively. The equation can be used to calculate the dynamic compressive yield strength of soft to medium-hard metals.

1. Introduction

Current research on pits produced in high-speed collisions includes: (a) the investigation of solid projectiles impinging against solid targets (artillery experiments); (b) the investigation of solid projectiles impinging against liquid surfaces (water entry problems); (c) the investigation of liquid drops impinging against solid surfaces (high-speed rain-erosion research); and (d) the investigation of liquid drops colliding with liquids. The work that is described in this paper was initiated as part of a high-speed rain-erosion research program and the entire program was conducted under the sponsorship of the Materials Laboratory, Directorate of Laboratories, Wright Air Development Center.

It is difficult to test for the rain-erosion resistance of structural materials at very high collision velocities because of the problems involved in accelerating either waterdrops or test specimens to the velocities in question. It has been suggested that it may be possible to bypass these problems by using drops of high-density liquids instead of drops of water for the erosion tests.[1] To develop this idea into a reliable test procedure, it is necessary to know the corresponding velocities-for-equal-damage when the test specimen collides with a drop of a high-density liquid and when it collides with a drop of water. The pit-depth-versus-velocity equation presented in this paper was developed to provide this information.

It has also been found that this pit-depth-versus-velocity equation is applicable without change to collisions of spheres of the soft, ductile metals with targets of the same metal in those cases in which the sphere flows as a result of collision with the metal plate when the collision velocity is as high as 5,000 ft/sec. Pellets of the soft, ductile metals appear, therefore, to behave as though they were liquid drops when they impinge against a solid surface at this velocity.

The experimental work reported in this paper was done in other laboratories.[2,3]

2. Collisions With Liquid Drops

The damage done to solid materials that collide at high speed with liquid drops depends both on the properties of a drop of liquid in collision and on the characteristic properties of the solid.

2.1. Damaging Properties of a Liquid Drop in High-Speed Collisions

As the relative collision velocity changes, the effects of collisions with a liquid drop also change. In high-speed collisions with the planar surface of a solid the liquid drop acts as though it were a hard solid sphere, but, unlike a sphere of hard solid material, it undergoes an ultrarapid radial flow outward about the point of impingement [1,2].[4] These damaging properties of an impinging liquid drop vary in intensity depending on the density of the liquid of the drop, on the relative collision velocity, and on the extent to which the solid surface yields under the blow. At any given impingement velocity, collision of a ductile metal plate with a liquid drop does not produce as deep a pit as collision of the same metal plate with a hard solid sphere would produce. This is because when a planar solid collides with a liquid drop part of the collision energy is transformed into the radial flow of the liquid.

[1] This idea was suggested by the rain-erosion research group working at Convair Division of General Dynamics Corp. in San Diego, Calif.

[2] The pit-depth-versus-velocity data reported for collisions of solid targets with liquid drops were obtained by the rain-erosion research group working at Convair Division of General Dynamics Corp.

[3] The pit-depth-versus-velocity data for collisions of spheres of the soft metals that flow as a result of the collision were obtained by Partridge, VanFleet, and Whited at the University of Utah (see reference [11].)

[4] Figures in brackets indicate the literature references at the end of this paper.

2.2. Response of Solid Target Materials

The extent and type of damage produced on solids as a result of collision with liquid drops depends strongly on the characteristic properties of the solids [1]. If the damage is to be described mathematically, it will be necessary to develop separate equations for the damage produced on solid materials that have widely different properties.

2.3. Dimensional Analysis of the Damage

To develop an equation that will give the depth of pits produced in high-speed collision between the planar surface of a solid and a liquid drop is a difficult problem from a theoretical standpoint. Dimensional analysis has proved to be a useful tool in the solution of difficult problems in the past. It is used in this paper to develop a pit-depth-versus-velocity equation.

The method of dimensional analysis has been discussed by Buckingham [3, 4], Bridgman [5], Birkhoff [6], and others. If a physical process can be described by physical quantities of n different kinds, and if none of the quantities involved in the process has been overlooked, then the process is described by the equation:

$$f(Q_1, Q_2, \ldots Q_n, r_1, r_2, \ldots)=0, \qquad (1)$$

where the Q's are the physical quantities involved in the process, and the r's are ratios. The Q's are quantities of different kinds. If several quantities of any one kind are involved in the process, they are specified by the value of any one of them, and by ratios of the others to this one. These ratios are the r's of eq (1).

A certain number k of the Q's are selected as fundamental. The k selected Q's comprise a possible set of fundamental dimensions and the remaining Q-quantities can be expressed in terms of them. After the k fundamental Q's, now designated as S's, have been selected, the remaining Q's are designated as P-quantities. In a mechanical system the number of the S-quantities is three because the total number of dimensions required to express any of the Q-quantities involved in a mechanical process is three. These dimensions are usually mass, length, and time.

Equation (1) may be put in the form

$$F(\pi_1, \pi_2, \ldots \pi_{n-k}, r_1, r_2, \ldots)=0, \qquad (2)$$

where the π's are independent products of the arguments Q, and are dimensionless in the fundamental units, or in the form

$$\pi_1=F'(\pi_2, \pi_3, \ldots \pi_{n-k}, r_1, r_2, \ldots) \qquad (3)$$

in which π_1 is any one of the π's.

A π-product is formed by multiplying each P-quantity by the S-quantities, which are raised to whatever powers α, β, . . . κ are required so that their units will just cancel those of the P-quantity to make the π-product dimensionless. That is,

$$\pi=(Q_1^{\alpha} \cdot Q_2^{\beta} \cdot \ldots Q_k^{\kappa})P. \qquad (4)$$

From a consideration of the equation for the pressure that results when a solid surface runs into a liquid drop at high speed [2], of the expression for the radius of flow of the liquid about the central point of the collision [2], and of the well known equation for the shear stress between layers of liquid in laminar flow, the quantities (see table 1) that should prove to be important in determining the damage that results from the collision of a solid surface with a liquid drop are: c, c', ρ, ρ', V, μ, γ, γ', d, and δ' where c is the speed of sound, ρ is the density, V is the relative impingement velocity, μ is the viscosity, $\gamma$is the surface tension, d is the diameter of the liquid drop, and δ' is the damage parameter. Primed quantities refer to the solid material; unprimed quantities refer to the liquid of the drop. In addition to these quantities there is the energy per unit volume put in, E', and the energy per unit volume returned, e', during the collision. E' is the energy per unit volume that the solid material can absorb without nonrecoverable deformation or fracture; e' is the energy per unit volume that the solid material can return. The ratio of these quantities, e'/E', is a measure of the resilience of the solid material.

TABLE 1. *The three fundamental S-quantities, the P-quantities, and the r-ratios involved in rain erosion damage*

Quantity	Dimensions	S	P	r	Dimensionless products, π
Impact velocity, V	L/T	S_1			
Drop diameter, d	L	S_2			
Density of liquid, ρ	M/L^3	S_3			
Viscosity of liquid, μ	M/LT	------	P_1	------	$\pi_1^{-1}=\rho dV/\mu$ Reynolds Number
Surface tension of liquid, γ	M/T^2	------	P_2	------	$\pi_2^{-1}=\rho dV^2/\gamma$ (Weber Number)^2
Velocity of sound in liquid, c	L/T	------	P_3	------	$\pi_3=c/V$ (Mach Number, liquid)$^{-1}$
Damage parameter, δ'	L	------	P_4	------	$\pi_4=\delta'/d$
Yield or rupture energy density of the solid, E'	M/LT^2	------	P_5	------	$\pi_5=E'/(\rho V^2)$
Ratio of sound velocities, c/c'	----------	------	------	r_1	
Ratio of densities, ρ/ρ'	----------	------	------	r_2	
Ratio of surface tension and interfacial tension, γ/γ'	----------	------	------	r_3	
Resilience, e'/E'	----------	------	------	r_4	

Of these quantities V, d, and ρ are arbitrarily selected to be the S-quantities, S_1, S_2, and S_3, respectively. Considering both these S-quantities and the remaining quantities, there are four pairs of quantities of the same kind: c, c'; ρ, ρ'; γ, γ'; and e', E'. These are expressed as four ratios, r_1, r_2, r_3, and r_4, respectively. One member of each of these pairs is a P-quantity if it has not already

been chosen to be an S-quantity. Also any other of the tabulated quantities that has neither been expressed in a ratio nor chosen to be an S-quantity is a P-quantity. The P-quantities are then:

$$\mu,\ \gamma,\ c,\ \delta',\ \text{and}\ E'\ (\text{see table 1}).$$

The π-products are formed by multiplying the P-quantities by the product of powers of the S-quantities. Each S-quantity is raised to whatever power is required to make the π-product dimensionless. For example, the viscosity μ has the dimensions $M/(LT)$ where M is mass, L is length, and T is time, and, therefore:

$$\pi_1^{-1}=\rho\ d\ V/\mu=(M/L^3)\ (L)\ (L/T)\ (LT/M). \quad (5)$$

Surface tension γ has the dimensions M/T^2 and, therefore,

$$\pi_2^{-1}=\rho\ d\ V^2/\gamma=(M/L^3)\ (L)\ (L^2/T^2)\ (T^2/M). \quad (6)$$

π_3, π_4, and π_5 are formed by a similar procedure. π_1^{-1} and π_2^{-1} are the dimensionless Reynolds Number and the square of the Weber Number, respectively. π_3^{-1} is a kind of Mach Number that gives the ratio of the relative impact velocity between the liquid drop and the solid surface to the speed of sound in the liquid of which the drop is composed.

The damage parameter δ' may be chosen to be a length, a volume, or an area. A length is the easiest quantity to measure experimentally. Taking δ' to be a length, eq (3) for the damage caused by high-speed collision of a solid surface with a liquid drop is

$$\delta'/d=F'[\rho dV/\mu,\ \rho dV^2/\gamma,\ V/c,\ E'/(\rho V^2),\ c'/c,$$
$$\rho'/\rho,\ \gamma'/\gamma,\ e'/E']. \quad (7)$$

It was pointed out in section 2.2 that it will be necessary to develop separate equations to describe the damage produced in liquid-drop-solid-surface collisions for materials that have widely different properties. The damage produced on nonrubbery materials that fail by plastic yield but without fracture is the easiest case to consider. It includes materials such as the soft and medium hard metals. If the collision velocity is not too high, the damage marks produced on these materials by high-speed collision with liquid drops are empty spheroidal segments. Surface and cross-sectional views of such pits in collision experiments performed elsewhere[2] are shown in figures 1, 2, and 3.

The damage pits produced in the planar surface of soft and medium hard metals when the leading surface of the solid runs into a liquid drop at high speed are almost exclusively due to the impact pressure produced. Although the radial flow of the liquid does make a contribution to the damage in the case of the soft metals (it drags metal up the walls of the damage pit and piles it up at the mouth of the crater), this contribution may be small enough in comparison with the damage that is caused by the pressure so that it can be neglected in first approximation. Neglecting all the dimensionless products that result from consideration of the radial flow of the liquid drop and from resilience of the solid target material, the approximate dimensionless damage equation for this class of materials is

$$\delta'/d=F'[\rho'/\rho,\ c'/c,\ V/c,\ E'/(\rho V^2)], \quad (8)$$

where δ' is the depth of the damage pits.

2.4. Experimental Observations

Graphs of measured values of pit depth plotted against relative collision velocity indicate that in the velocity range that has been investigated the pit-depth-versus-velocity curve is very close to a straight line regardless of whether the pits were caused by firing steel spheres against a stationary specimen plate or by firing a specimen plate at high velocity against relatively stationary liquid drops. It is to be expected that at a fixed relative collision velocity the depth of pit caused by a projectile that does not flow during the collision (hardened steel sphere) will be deeper than that caused by a projectile that does flow during the collision (liquid drop). In the first case all of the kinetic energy (neglecting that which is converted into heat) is delivered to the solid target; in the second case part of the kinetic energy is used to produce the flow of the projectile and only the remainder is delivered to the solid target.

Experiments in which 7/32-in. steel spheres were fired against 1/8-in.-thick type-1100 aluminum plates have been carried out by Mr. Herschel L. Smith at the Naval Research Laboratory, Washington, D.C. Some of the data obtained in these experiments are presented in figure 4. One important fact is apparent from these data, namely, for the sphere diameter and for the thickness of specimen plate used, if the specimen plate has only peripheral support the pit-depth-versus-velocity curve has an intercept on the velocity axis, but if the specimen plate is rigidly backed by a heavy steel supporting plate the pit-depth-versus-velocity curve goes directly to the origin.

Experiments in which target plates of different metals were fired into drops of mercury and drops of water at high speed have been carried out in another laboratory.[2] Some of the data obtained are plotted in figures 5 and 6. It can be seen that in every case the pit-depth-versus-velocity curve is essentially a straight line with an intercept on the velocity axis. From the bulge on the trailing face of the specimen in picture 6 of figure 2 it is apparent that the metal plates are supported during the collision with the liquid drops in such a way that the trailing face of the target plate is a free surface. An important fact apparent from the data plotted in figure 6 is that the slope of the straight line is a function of the drop size.

On the basis of the evidence presented, if the specimen has peripheral support only, the pit-depth-

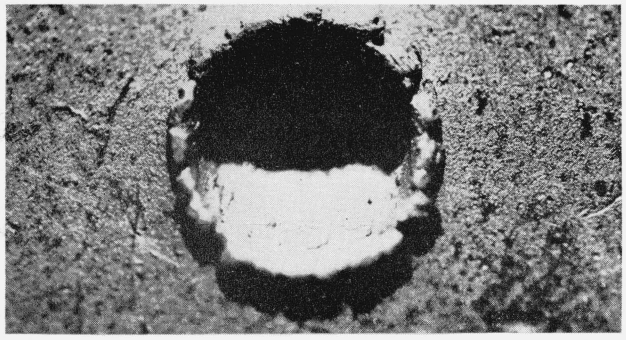

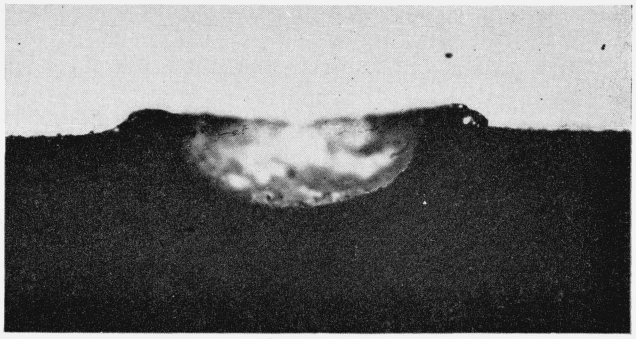

1 SURFACE VIEW 4 CROSS—SECTIONAL VIEW

IMPINGEMENT VELOCITY 686 ft/sec

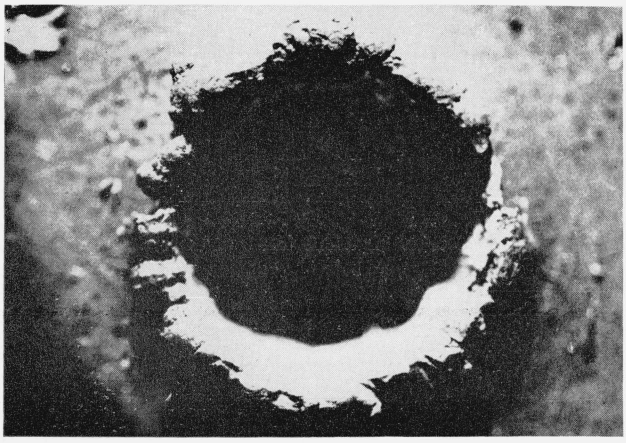

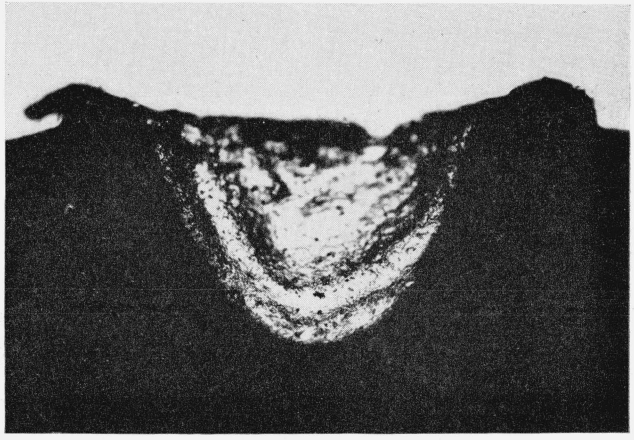

2 SURFACE VIEW 5 CROSS—SECTIONAL VIEW

IMPINGEMENT VELOCITY 1250 ft/sec

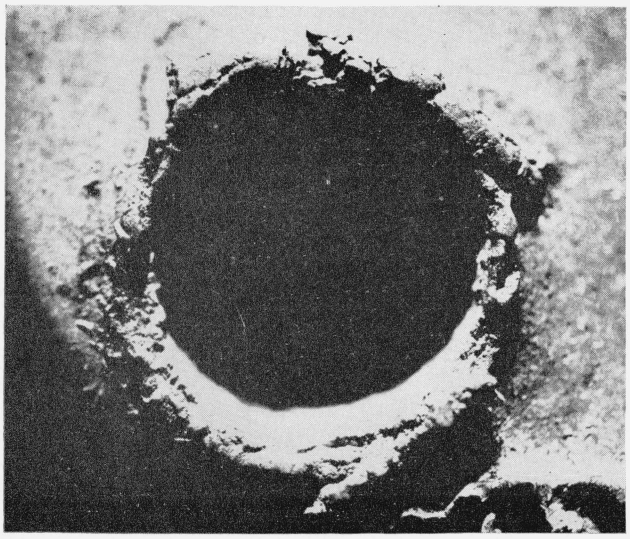

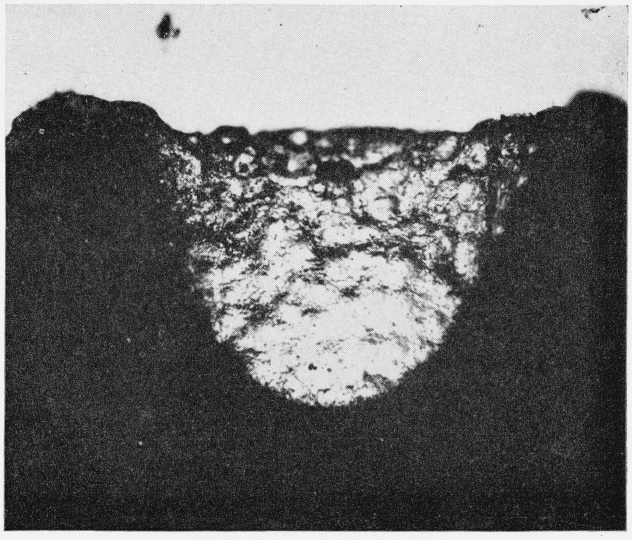

3 SURFACE VIEW 6 CROSS—SECTIONAL VIEW

IMPINGEMENT VELOCITY 1645 ft/sec

FIGURE 1. *Mercury-drop damage pits in lead.*

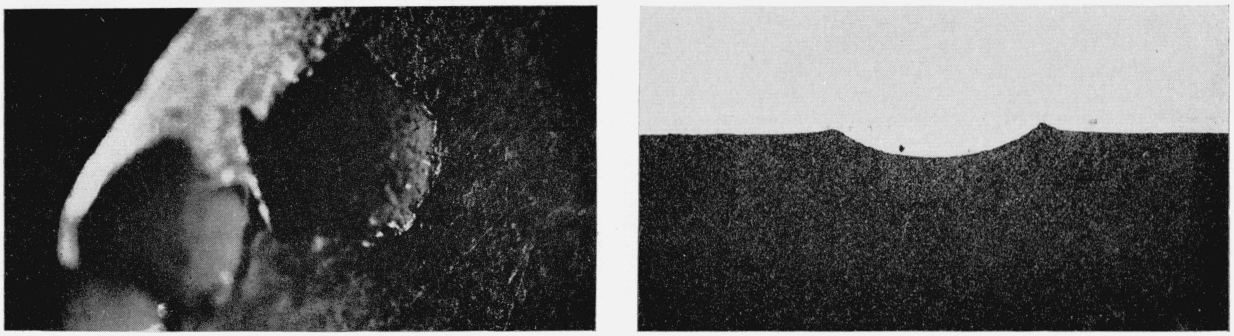

1 SURFACE VIEW 4 CROSS—SECTIONAL VIEW

IMPINGEMENT VELOCITY 686 ft/sec

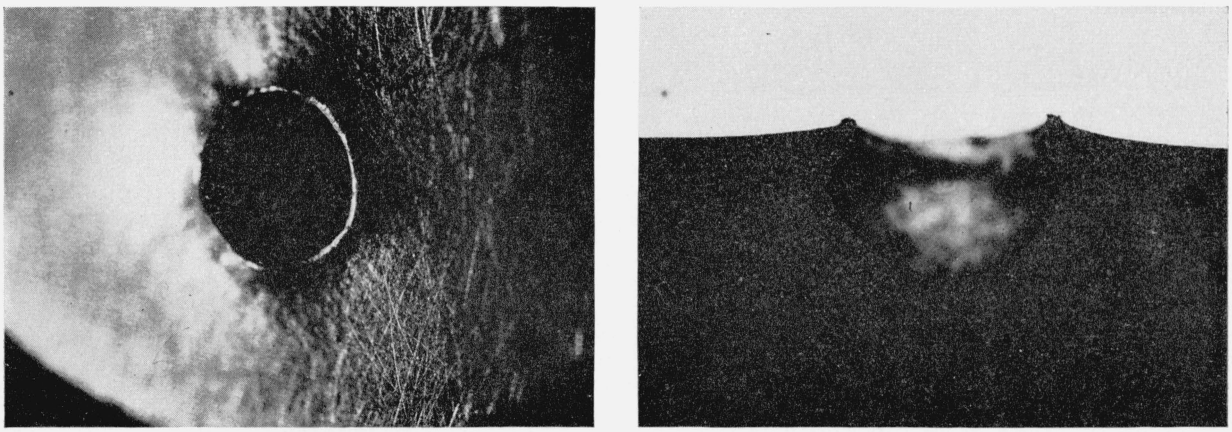

2 SURFACE VIEW 5 CROSS—SECTIONAL VIEW

IMPINGEMENT VELOCITY 1285 ft/sec

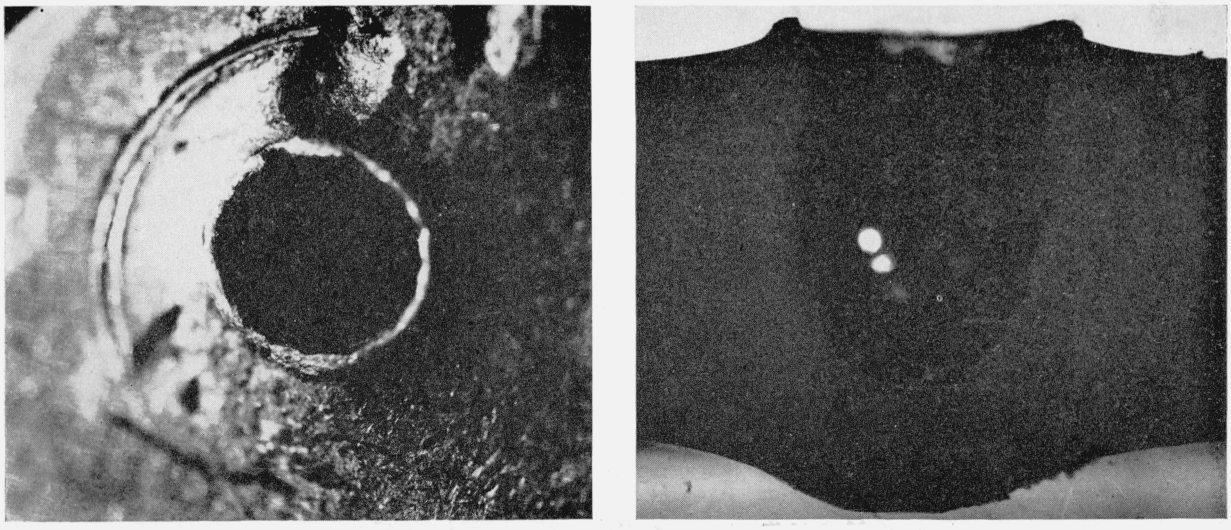

3 SURFACE VIEW 6 CROSS—SECTIONAL VIEW

IMPINGEMENT VELOCITY 2320 ft/sec

FIGURE 2. *Mercury-drop damage pits in 1100 aluminum.*

1 SURFACE VIEW

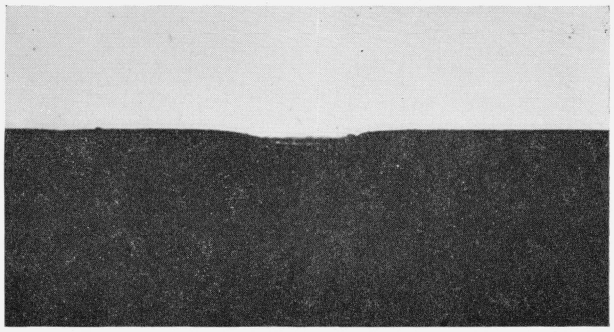

4 CROSS—SECTIONAL VIEW

IMPINGEMENT VELOCITY 695 ft/sec

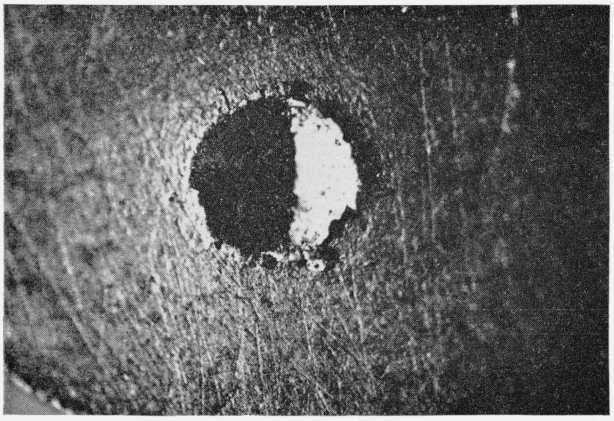

2 SURFACE VIEW

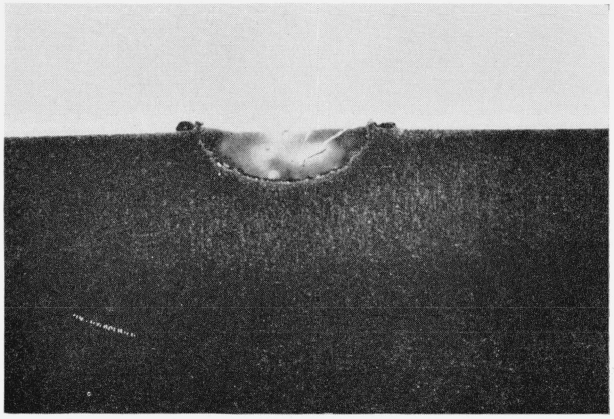

5 CROSS—SECTIONAL VIEW

IMPINGEMENT VELOCITY 1200 ft/sec

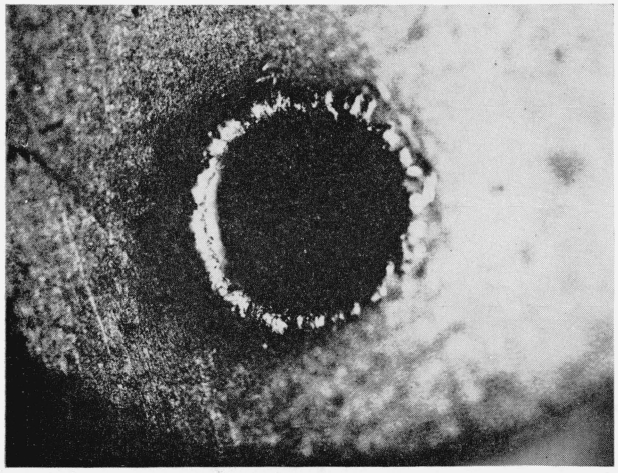

3 SURFACE VIEW

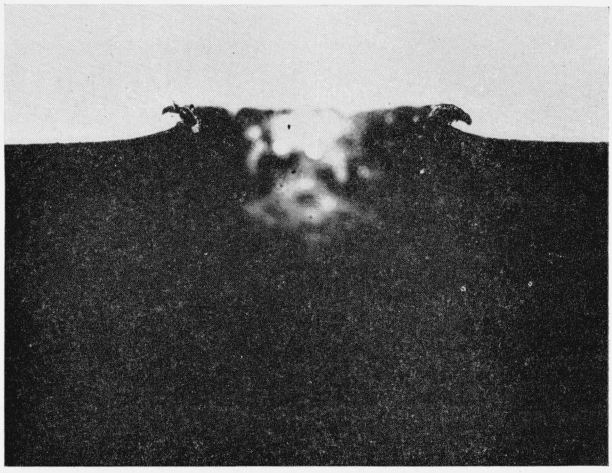

6 CROSS—SECTIONAL VIEW

IMPINGEMENT VELOCITY 2445 ft/sec

FIGURE 3. *Mercury-drop damage pits in copper.*

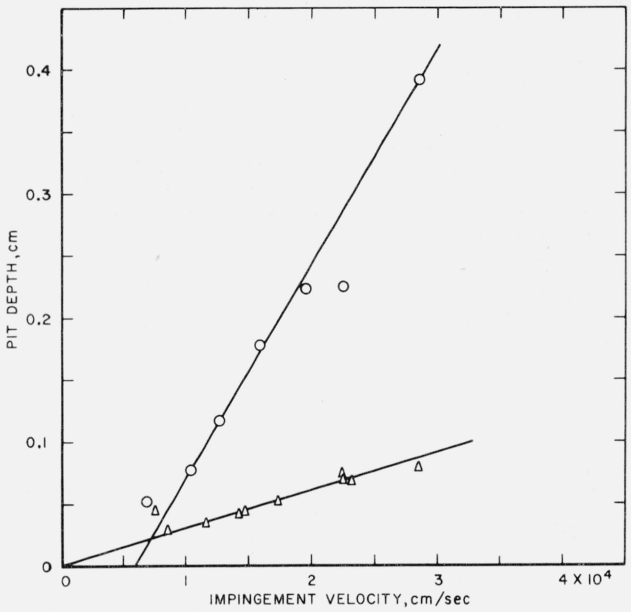

FIGURE 4. *Best-fit curves for collisions of 0.55-cm steel spheres against plates of 1100 aluminum.*

⊙ aluminum plate with edge support only; △ aluminum plate rigidly clamped to heavy steel plate.

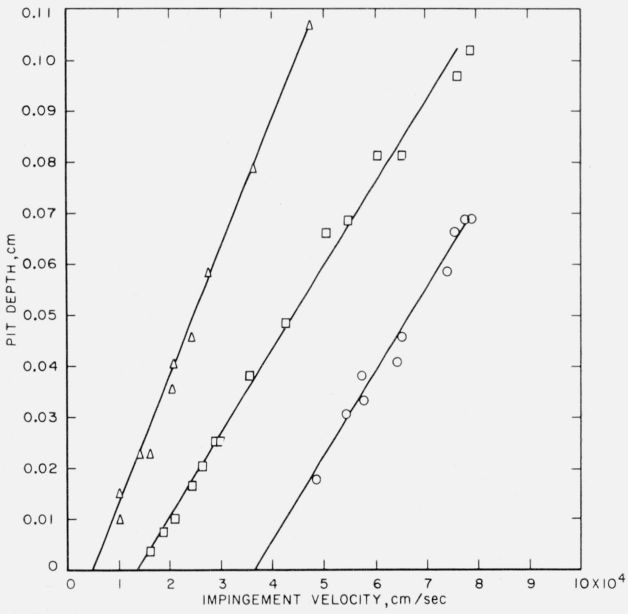

FIGURE 5. *Best-fit curves for collisions of mercury drops against plates of three different metals.*

△ 0.10-cm mercury drops against lead; ⊡ 0.10-cm mercury drops against copper; ⊙ 0.15-cm mercury drops against iron.

versus-velocity equation for materials of the response type being considered appears to be:

$$\delta' = K_1 V - K_2, \tag{9}$$

where K_1 and K_2 are constants.[5] It appears that

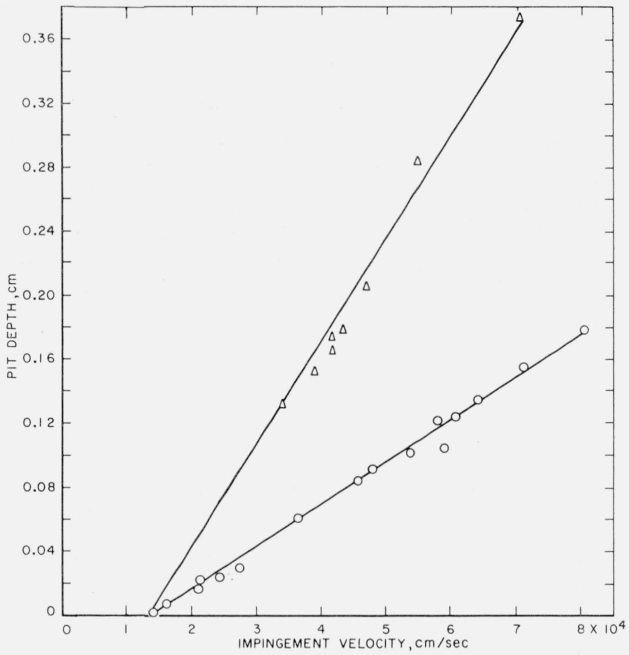

FIGURE 6. *Best-fit curves for collisions of mercury drops of two sizes against plates of 1100 aluminum.*

⊙ 0.10-cm mercury drops; △ 0.20-cm mercury drops.

this equation applies regardless of whether the pits are produced by the impingement of solid projectiles against solid targets or by firing solid target plates into liquid drops at very high velocities. However, because the amount of the kinetic energy delivered to the target depends upon whether or not the projectile flows during the collision, the constants K_1 and K_2 will be different for solid-target-versus-solid-projectile and for solid-target-versus-liquid-projectile collisions.

2.5. Pit-Depth-Versus-Velocity Equation for Medium-Thin Metal Targets

For targets that are metal plates, that have a thickness several times the diameter of the projectile, and that are mounted so that the reverse side of the plate is a free surface, a pit-depth-versus-velocity equation can be developed by considering the movement of a cylindrical core of material through the target plate under the area of contact involved during the collision. If the target plate is fired against the projectile, this core of target material is slowed down with respect to the remainder of the target plate as a result of the collision and there is a relative motion between this core and the remainder of the target plate, which moves forward with respect to it.

[5] Partridge, VanFleet, and Whited [11] also reported a linear relationship between pit depth and velocity; the linear relationship was established independently by the author on the basis of the Convair data.

If the reverse side of the target plate is a free surface and the core can move *freely* with respect to the remainder of the plate, the kinetic energy transformed as a result of the collision is largely converted into the work of moving the core against the bonding that holds it to the remainder of the target plate. For these conditions there is an intercept on the velocity axis. In terms of this model, it would appear that the intercept velocity is related to the shear yield strength of the material of the target plate. In the range of velocities that are just in excess of the threshold velocity required to produce any permanent damage at all (intercept velocity), it appears that the core may only be displaced with respect to the remainder of the target plate. For this case plastic deformation occurs only at the cylindrical boundary of the core. At higher velocities plastic deformation may occur within the core itself.

Consider that a small target plate moving at velocity V in a stationary coordinate system, which is located outside of the target plate, strikes a stationary liquid drop (see fig. 7). The result of the collision is that a wave of compression is initiated both in the solid material of the target plate and in the liquid of the drop. It is helpful to view the collision incident as it is seen by an observer located at the origin of the coordinate system in figure 7. This observer sees a target plate, all parts of which are moving forward uniformly at velocity V in the $(+y)$-direction, approach a spherical drop, all parts of which are stationary. After the collision has occurred, the observer sees a zone in which the particles of the material of the target plate have taken on a velocity, aV, in the $(-y)$-direction where a is a constant; this zone is indicated schematically with a dotted line and the letter A in figure 7. Similarly, the observer sees a zone in the liquid drop in which the particles of the liquid have taken on a velocity, bV, in the $(+y)$-direction where b is a different constant; this zone is indicated schematically with a dotted line and the letter B in figure 7. Zone A spreads at the characteristic sound velocity of the target material, c', through the thickness, d', of the target plate and zone B spreads at the characteristic sound velocity, c, of the liquid of which the drop is composed, through the diameter, d, of the liquid drop.

To the observer who looks first at a point A' that is in the target plate but outside the spreading boundary of zone A and who then looks at the material within zone A, it appears that the particles at A' have a velocity V and that the particles in zone A have a velocity $(1-a)V$. After a time t that is just long enough for zone A to complete one trip through the thickness of the target plate, the leading surface of the target plate at point A' in figure 7 has advanced a distance Vt, but in the same time t the area of the leading surface of the target plate that constitutes the upper boundary of zone A in figure 7, has advanced only by $(1-a)Vt$. If the average negative velocity of the core is taken to be $aV/2$, the displacement that exists between the leading surface of the target plate at point A' and the upper boundary of zone A after time t is $aVt/2$.

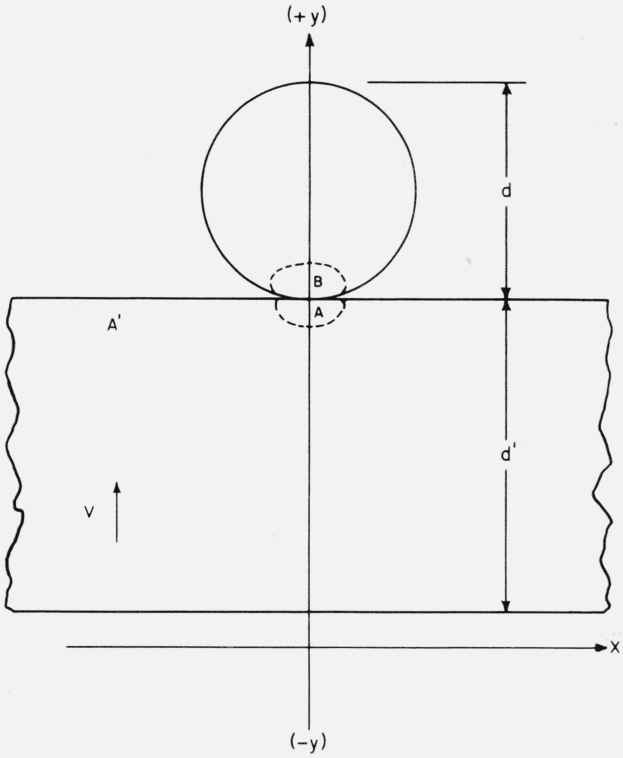

FIGURE 7. *Stationary coordinate system for a liquid-drop-versus-solid-specimen collision.*

If the observer watches zone B as it just spreads to the opposite side of the liquid drop, he sees that this zone reflects from the free air-liquid interface with change of sign, that is, he sees a tension wave begin to move toward him in the $(-y)$-direction of figure 7. Within the tension wave the particle velocity is $2bV$ in the $(+y)$-direction. The tension wave moves toward the observer at the characteristic speed of sound, c, of the liquid of which the drop is composed. In the zone of the liquid of the drop that has been traversed by the tension wave the particles of the liquid are unstressed and are moving at velocity $2bV$ in the $(+y)$-direction. At the instant that the tension wave returns to the collision surface, where radial flow of the liquid of the drop is occurring, all of the liquid of the drop is unstressed and moving at the velocity $2bV$ in the $(+y)$-direction.

It can be assumed that return to the collision surface of the tensile wave in the liquid provides a cutoff for the collision. At this instant all of the liquid of the drop is unstressed. The collision surface will appear to be a free surface to the compressed particles of the material of the target plate in zone A. A wave of relief (tension) will then be initiated in the material of the target plate and will begin to trail zone A which continues to spread through the thickness, d', of the target plate.

Let the arbitrary time t referred to previously now be the time that is required for zone B to make one round trip through the liquid drop. Then $t=2d/c$. The distance to which zone A has spread in this time is $c't$ and this determines the length of the compressed zone A which continues to move through the target plate. When zone A reaches the free trailing surface of the target plate, it also reflects as a tension wave. This tension wave moves in the $(+y)$-direction of figure 7. In that part of zone A that has been traversed by the returning tension wave the particles of the material of the target plate are under zero stress and have velocity $(1-2a)V$ in the $(+y)$-direction. When the reflected tension wave in the target plate reaches the leading surface of the plate it undergoes partial reflection back into the material of the target plate and partial transmission into the liquid of the drop which is running off radially around the central point of the collision.

a. Slope of the Pit-Depth-Versus-Velocity Curve

The compressional wave spreads slightly as it moves through the thickness of the target plate; consequently, the core of material through the target plate that is slowed down as a result of the collision is in reality somewhat conical in shape. For simplicity, the true situation may be idealized in two ways. First, the core may be regarded as a true cylinder which is free to move or slide in the direction of the collision blow but which is restrained laterally. A similar cylinder exists in the liquid of which the drop is composed. Secondly, the compressional waves that move through the cylinder in the target plate and through the cylinder in the drop may be regarded as plane waves.

For the case of plane waves, $a=z/(z+z')$ and $b=z'/(z+z')$ where $z=c\rho$ and $z'=c'\rho'$ are the acoustic impedances of the material of the drop and of the material of the target plate, respectively. The relations are found by equating the plane-wave stress in the material of the drop, σ, to the plane-wave stress in the material of the target plate, σ', that is,

$$\sigma=c\rho v=c'\rho'v'=\sigma', \tag{10}$$

where v, v' are the particle velocities in the zones traversed by the compressional waves initiated in the drop and in the target plate, respectively, and by imposing the condition that the impacting surfaces remain in contact, namely,

$$v+v'=V. \tag{11}$$

From eq (10) and (11),

$$\begin{aligned} v'&=c\rho V/(c\rho+c'\rho') \\ &=zV/(z+z') \\ &=aV \end{aligned}$$

and

$$\begin{aligned} v&=z'V/(z+z') \\ &=bV. \end{aligned} \tag{12}$$

This derivation is the same as that for the collision of two free rods except that, for the case that the rods are cylinders that are free to move in the collision direction but that are restrained laterally, the sound speed that must be used is the speed of sound in an infinite medium. This can be shown as follows.[6] According to Hooke's law:

$$E\epsilon_l=\sigma_l-\nu(2\sigma_r)=\sigma_l-2\nu\sigma_r, \tag{13}$$

where E is Young's modulus, ϵ_l is the longitudinal strain, σ_l is the longitudinal stress, ν is Poisson's ratio, and σ_r is the radial stress. Also,

$$E\epsilon_r=\sigma_r-\nu(\sigma_l+\sigma_r)=0, \tag{14}$$

where ϵ_r is the radial strain. From eq (14),

$$\sigma_r=\nu\sigma_l/(1-\nu). \tag{15}$$

By substituting the expression for σ_r given by eq (15) into eq (13) it is found that

$$\sigma_l=\frac{(1-\nu)E\epsilon_l}{(1-2\nu)(1+\nu)}, \tag{16}$$

and because, for plane waves, $c=[\sigma_l/\rho\epsilon_l]^{1/2}$

$$c=\left[\frac{(1-\nu)}{(1-2\nu)(1+\nu)}\ \frac{E}{\rho}\right]^{1/2}. \tag{17}$$

This is the sound speed for an infinite medium and it is the sound speed that must be used both for c and for c' in the expressions for a and for b.

The depth of pit produced at any relative impingement velocity is proportional to the negative velocity produced in the cylindrical core in the target plate as a result of the collision and to the time that this negative velocity exists. If it is assumed that the elastic wave that is induced in the cylindrical core as a result of the collision makes a round trip through the core in the time interval $2d/c$, then, at the end of this time interval, the cylindrical core is moving as a rigid body and the negative velocity that it has acquired with respect to the remainder of the target plate is given approximately by $2zV/(z+z')$. During this time interval the average negative velocity given to the material of the cylindrical core was $zV/(z+z')$. The slope K_1 of eq (9) is then $k_1(2d/c)\ [z/(z+z')]$ where k_1 is a new constant.

The experimental data for a number of target metals of widely different properties fired against drops of mercury, and for three target metals fired both against drops of mercury and drops of water, require that $k_1=3.6$. Because this value of the constant k_1 brings the calculated curve into good agreement with the experimental data for a number of target metals and for two drop liquids, it would appear that k_1 does not involve properties either of

[6] The author is indebted to Dr. John M. Frankland of NBS Mechanics Section for the proof in elasticity theory that it is the sound speed in infinite medium that is required.

the material of the target plate or of the liquid of the drop. Therefore, eq (9) is

$$\delta'=7.2d\left(\frac{z}{z+z'}\right)\left(\frac{V}{c}\right)-K_2. \tag{18}$$

Substitution of $z=c\rho$, $z'=c'\rho'$, and division by d puts eq (18) in the dimensionless form

$$\frac{\delta'}{d}=\frac{7.2}{1+\left(\frac{c'}{c}\right)\left(\frac{\rho'}{\rho}\right)}\left(\frac{V}{c}\right)-K_2/d, \tag{19}$$

where K_2/d is a dimensionless intercept. Four of the dimensionless quotients predicted by eq (8) are found in eq (19).

b. Intercept on the Velocity Axis

The process previously postulated, namely, that the core of target material below the collision area is slowed down with respect to the remainder of the target plate so that the remainder of the target plate moves forward with respect to it, certainly occurs at all impingement velocities. However, no observable damage pit is produced at all below a critical velocity, and, if the liquid of the drop is kept constant, this critical velocity is different for each of the metals for which data are available. (See fig. 5.) The intercept velocity is also different on the same metal if the liquid of the drop is changed.

The fact that no permanent damage pit is formed below a given velocity which is characteristic for each metal, indicates that for velocities lower than this critical velocity the relative motion between the core and the remainder of the target plate is completely elastic and that no permanent shear deformation occurs in the material around the cylindrical wall of the core. The intercept of the pit-depth-versus-velocity curve appears to be a function of the shear yield strength of the material, that is, of the remaining dimensionless quotient $E'/(\rho V^2)$ of eq (8) taking E', the energy per unit volume absorbed by the target material without fracture or plastic yield, to be the shear yield strength.

It has been pointed out that the experimental pit-depth-versus-velocity curve is a straight-line function of the velocity. Therefore, the dimensionless quotient $E'/(\rho V^2)$ cannot be used for the intercept without eliminating the factor $1/V^2$. This can be accomplished by multiplying the dimensionless quotient $E'/(\rho V^2)$ by the square of the dimensionless quotient V/c of eq (8) to obtain $E'/(\rho c^2)$. If this expression is substituted for the dimensionless intercept K_2/d in eq (19) and if the intercept condition that $\delta'/d=0$ is imposed, the expression that is found for the intercept velocity is not able to account for the observed ratio of experimental intercepts. It was found that the observed intercept velocities can be accounted for if the dimensionless quotient $E'/(\rho c^2)$ is multiplied by the dimensionless quotients $(\rho/\rho')^{1/2}$, z/z', c/c', and by a dimensionless numerical constant, k_2, having the value 136.8. Substitution of the resulting dimensionless quotient, 136.8 $E'z/(\rho^{1/2}\rho'^{1/2}cc'z')$, for the dimensionless intercept, K_2/d, in eq (19) and use of the acoustic impedance z for $c\rho$ produces the dimensionless pit-depth equation

$$\frac{\delta'}{d}=\frac{7.2z}{z+z'}\left(\frac{V}{c}\right)-\frac{136.8E'z}{\rho^{1/2}\rho'^{1/2}cc'z'}. \tag{20}$$

If the intercept condition that $\delta'/d=0$ is imposed, the intercept velocity, V_i, is found to be given by

$$V_i=\frac{19E'(z+z')}{(\rho c'z'^3)^{1/2}}. \tag{21}$$

It is noteworthy that one would expect V_i to be given by $E'(z+z')/zz'$ multiplied by some constant, because the plane wave stress is given by $zz'V/(z+z')$. It was found, however, that this expected expression would not give the observed intercept velocities for both mercury drops and waterdrops if the same numerical constant was used for both drop liquids. Equation (21) appears at present to be the best expression for the intercept velocity. When more data are obtained and the problem is studied further, it may be found necessary to change it.

The numerical constants in eqs (20) and (21) have been chosen to give best fit to the pit-depth-versus-velocity data. The values used for the physical constants of the different materials are given in table 2. In choosing the constants, the speed of sound in infinite medium was used for c' and the dynamic compressive yield strength was used for E'. (In liquids there is only one speed of sound that can be used for c.) Dynamic rather than static strength values must be used for E' because the loading time is of the order of several microseconds. The strength that should be used for E' is the dynamic yield strength in shear. Unfortunately, the amount of work that has been done in determining the dynamic yield strengths of materials is very limited. Whiffin [7] has determined the dynamic yield strength in compression for a number of materials. In choosing the numerical constant for eq (21), the dynamic yield strength in compression was used for E' instead of the dynamic yield strength in shear. Some justification for this substitution may be found in the Von Mises strain energy theory according to which the tensile elastic limit, σ_y, is $\sqrt{3}\ \tau_y$ where τ_y is the yield strength in shear.

2.6. Test of the Equation

For pit-depth calculations, eq (20) may be put in the form

$$\delta'=\frac{7.2\ d\ z}{c(z+z')}\,[V-V_i], \tag{22}$$

where V_i is the intercept velocity for the particular liquid-drop-solid-target combination being used and where V_i is given by eq (21). Pit-depth-versus-velocity data obtained in another laboratory[2] were used to test the equations. In most cases the

TABLE 2. *Physical Constants*

Metal	Density, ρ	Sound speed, c (infinite medium)	Acoustic impedance, z	Static tensile yield strength, Y	Dynamic compressive yield strength, E'
	g/cm³	*cm/sec*	*g/sec-cm²*	*psi*	*d/cm²*
1100–0 aluminum	[a] 2.713	[d] 6.318×10^5	1.714×10^6	[f] 2,625 [c] 5,000	[g] 7.239×10^8 [h] 1.183×10^9
2024–0 aluminum	[a] 2.768	[d] 6.370×10^5	1.763×10^6	[f] 12,625	[g] 2.350×10^9
Copper, annealed electrolytic tough pitch	[b] 8.92	[d] 4.691×10^5	4.184×10^6	[f] 3,975	[h] 2.394×10^9
Lead, chemical	[b] 11.3437	[d] 2.277×10^5	2.583×10^6	----------	[h] 4.324×10^8
Lead, pig	----------	[d] 2.128×10^5	2.414×10^6	----------	----------
Steel, cold rolled	[c] 7.859	[d] 5.786×10^5	4.547×10^6	----------	[i] 8.274×10^9
Iron	[b] 7.86	[e] 5.850×10^5	4.598×10^6	----------	[h] 7.660×10^9
Zinc	[b] 7.14	[e] 4.170×10^5	2.977×10^6	----------	----------
Mercury	[b] 13.546	[e] 1.451×10^5	1.966×10^6	----------	----------
Water, 25° C	[b] 0.99707	[e] 1.497×10^5	0.1493×10^6	----------	----------

[a] Data from Aluminum Co. of America.
[b] Data from Handbook of Chemistry and Physics.
[c] Data from Metals Handbook, 1948.
[d] Measured in NBS Sound Section by Carroll Tschiegg.
[e] Data from L. Bergmann [12].
[f] Measured in NBS Engineering Mechanics Section by Lafayette K. Irwin.
[g] Data of A. C. Whiffin, communicated by letter.
[h] Data of A. C. Whiffin [7].
[i] Extrapolated from graph, figure 7e, given by Krafft and Sullivan [9].

physical properties of the metals used in the experiments were not determined. The physical constants used for these materials in eqs (21) and (22) are given in table 2.

a. Test of the Equation With Mercury Drops and Pure Metal Targets

Pit-depth-versus-velocity curves calculated by eq (22) for collisions of 0.10- and 0.15-cm mercury drops against copper are shown in figure 8. Experimental points for the two drop sizes are indicated in this figure with circles and with triangles, respectively. The material used in these experiments[2] was described as pure copper. Physical constants for electrolytic copper were used in the calculations. The intercept velocity, V_i, was calculated by use of eq (21). It can be seen that both the slope and intercept of the calculated curves are in good agreement with the experimental data.

Pit-depth-versus-velocity curves calculated by use of eq (22) for collisions of 0.10-, 0.15-, and 0.285-cm mercury drops against 1100-0 aluminum are shown in figure 9. Experimental points for the three drop sizes that were used are indicated in this figure with circles, triangles, and squares, respectively. The intercept velocity, V_i, was calculated by use of eq (21). The value of the dynamic compressive yield strength that was used for E' in eq (21) was calculated by means of a formula given by Whiffin [7] for the Duralumins. The static yield strength of the 1100–0 aluminum used was not known.[2] For the purpose of the calculation of E' it was taken to be 5,000 psi (table 2). The speed of sound in infinite medium, determined for a piece of 1100–0 aluminum of lower yield strength by Tschiegg (table 2) was used for c' and in computing z'. There is more scatter in the experimental data for the 0.15-cm drop size than for the other two drop sizes. Scatter could be caused by variation of the drop size from the reported value; it could also be caused by use of target plates cut from sheet material of different yield strength. The data for both the 0.15-cm and 0.285-cm drop sizes would fit the curves better if the intercept velocity were 1.1×10^4 cm/sec rather than 1.26×10^4 cm/sec, which was the value found by use of eq (21). The experimenters report [8] that the target plates were cut from 1100-aluminum sheets having thicknesses in the range of 0.185 to 0.210 in.; hence, they were not all cut from the same sheet stock and, consequently, some variation in yield strength, which would affect the intercept velocity directly, could have been present. In general, however, there is good agreement between the experimental data and the calculated curves.

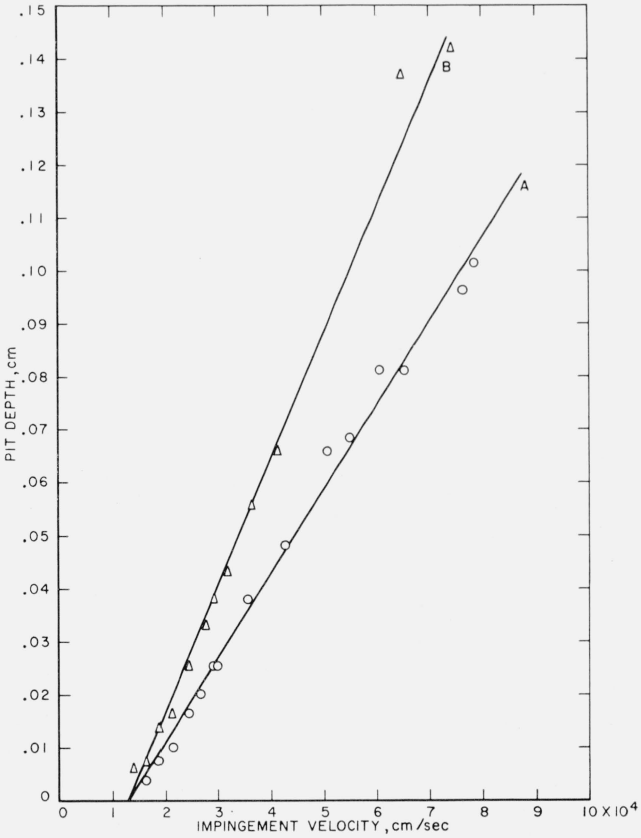

FIGURE 8. *Calculated curves for collisions of mercury drops of two sizes against plates of copper.*

⊙ observed depth for 0.10-cm drop; A, calculated curve for 0.10-cm drop; △ observed depth for 0.15-cm drop; B, calculated curve for 0.15-cm drop.

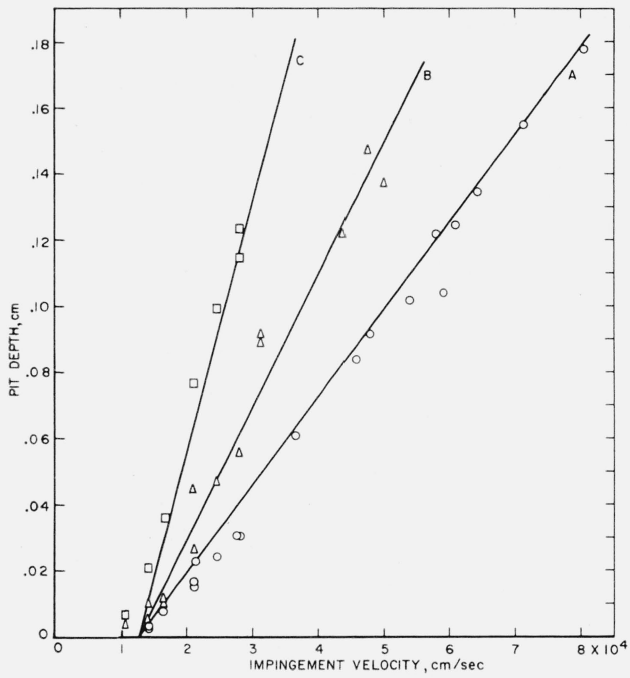

FIGURE 9. *Calculated curves for collisions of mercury drops of three sizes against plates of 1100 aluminum.*

⊙ observed depth for 0.10-cm drop; A, calculated curve for 0.10-cm drop; △ observed depth for 0.15-cm drop; B, calculated curve for 0.15-cm drop; ⊡ observed depth for 0.285-cm drop; C, calculated curve for 0.285-cm drop.

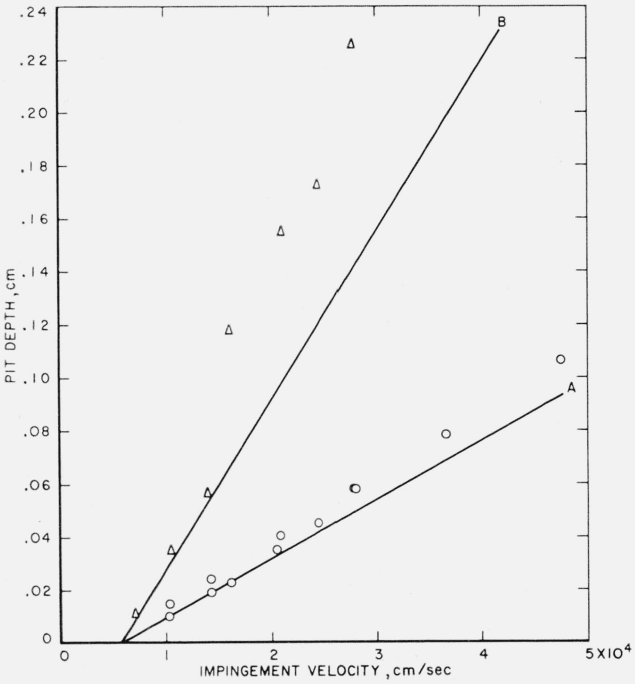

FIGURE 10. *Calculated curves for collisions of mercury drops of two sizes against lead target plates.*

⊙ observed depth for 0.10-cm drop; A, calculated curve for 0.10-cm drop; △ observed depth for 0.285-cm drop; B, calculated curve for 0.285-cm drop.

The pit-depth-versus-velocity curves calculated by use of eq (22) for collisions of 0.10-cm and for 0.285-cm mercury drops against lead are shown in figure 10. The experimental points for the two drop sizes are indicated with circles and with triangles, respectively. The intercept velocity, V_i, was calculated by use of eq (21). The value of the dynamic compressive yield strength used for E' in eq (21) was that given for 99.97 percent lead by Whiffin (table 2). The value of the speed of sound in infinite medium for pig lead measured by Tschiegg (table 2) was used for c' and in computing z'. The calculated curves are a good fit to the data at the lower velocities; at the higher velocities the depth of the pits is greater than that predicted by eq (22). The pits produced in lead by mercury drops are characterized by a heavier lip of metal around the mouth of the crater than is observed on pits in 1100–0 aluminum or on pits in copper. See figures 1, 2, and 3. It appears that for a metal that is as soft as lead the flow of a liquid-drop projectile at high collision velocities drags a notable amount of metal from the bottom of the pit and piles it up at the mouth of the crater. This extra mode of pit formation was neglected in the development of eq (22) and, therefore, this equation does not fully account for the depth of pits formed at very high velocities in metals as soft as lead.

b. Test of the Equation With Mercury Drops and Alloy Metal Targets

Experimental pit-depth-versus-velocity data were obtained for collisions of 0.15-cm mercury drops with steel targets in another laboratory.[2] It was reported that the target material was originally ¾H cold-rolled steel. After annealing above the alpha temperature it developed a case hardening. The case hardening was chipped off and the target plates were polished. It was reported that the resulting material had an average Rockwell E hardness of 90.96 and Brinell hardness of 90.98, which they stated corresponds to an ultimate tensile strength of 47,200 psi.

In order to calculate the intercept velocity by means of eq (21) it is necessary to know the dynamic compressive yield strength of the target metal. The manganese and carbon contents of steels strongly affect their dynamic yield strength; the manganese content is particularly important if it is low, for example, in the range from zero to 0.50 percent. A chemical analysis of the manganese and carbon content of one of the steel target plates was made in the NBS Analytical Chemistry Section. It revealed that the steel contained 0.70 percent manganese and 0.21 percent carbon. The value of the dynamic compressive yield strength used for E' in eq (21) was found by extrapolating a curve given by Krafft and Sullivan [9] for a steel containing 0.98 percent manganese and 0.22 percent carbon that was loaded in compression. The speed of sound in infinite medium determined for cold-rolled steel by Tschiegg (table 2) was used for c' and in computing z'.

The pit-depth-versus-velocity curve calculated by use of eqs (21) and (22) for collisions of 0.15-cm mercury drops against steel targets is shown in figure 11 along with the experimental points. It would appear that the intercept velocity is about correct. However, a straight line that would fit the experimental data would have a slope considerably less than that of the calculated curve. It would appear from this evidence that eq (22) does not predict pit depth with exactness for pits formed in targets of alloy steel.

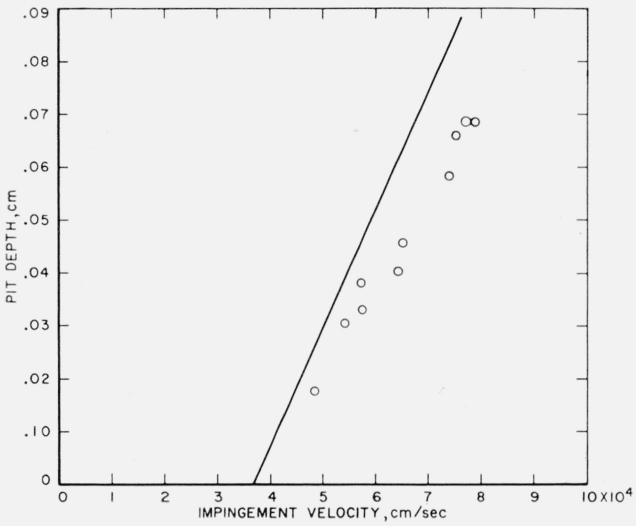

FIGURE 11. *Calculated curve for collisions of 0.15-cm mercury drops against steel.*

⊙ observed depth for 0.15-cm drop.

The pit-depth-versus-velocity curves calculated by use of eqs (21) and (22) for collisions of 0.10-cm and 0.20-cm mercury drops against 2024–0 aluminum targets are shown in figure 12 along with experimental points obtained elsewhere.[2] The experimental points for the two drop sizes are indicated with circles and triangles, respectively. The targets were prepared at the NBS. The average static yield strength (0.2% offset) of the metal used was found to be 12,625 psi from measurements made by Irwin (table 2). The dynamic compressive yield strength used for E' in eq (21) for this material was calculated from a ratio of the static to the dynamic yield strength of 2.7. This ratio was estimated by Whiffin [10] for the 2024–0 aluminum that was used for the targets. The speed of sound in infinite medium determined for 2024–0 aluminum by Tschiegg (table 2) was used for c' and in computing z'. The calculated curves differ from a best-fit line drawn through the experimental points in intercept but not in slope. If the intercept velocity had been 2×10^4 cm/sec rather than 2.421×10^4 cm/sec there would have been relatively good fit between the calculated curves and the experimental points.

In summarizing, it can be said that eqs (21) and (22) have not given calculated curves that show as

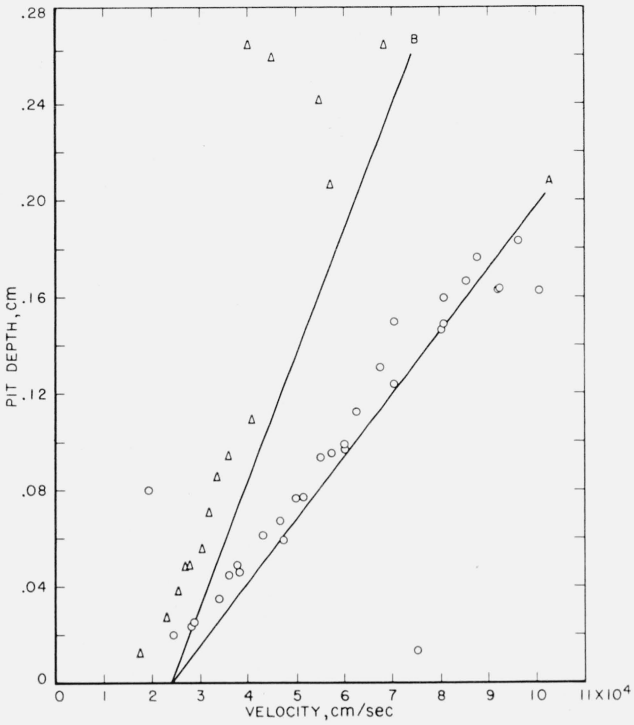

FIGURE 12. *Calculated curves for collisions of mercury drops of two sizes against target plates of 2024–0 aluminum.*

⊙ observed depth for 0.10-cm drop.
A, calculated curve for 0.10-cm drop.
△ observed depth for 0.20-cm drop.
B, calculated curve for 0.20-cm drop.

good agreement with experimentally determined points for collisions of target plates of alloy metals with mercury drops as that obtained for collisions of plates of pure metals with mercury drops.

c. Tests of the Equation With Waterdrops

Test results with waterdrops of constant size are available for some of the metals used in the experiments with mercury drops.

The pit-depth-versus-velocity curve calculated by use of eqs (21) and (22) for collisions of 0.2-cm waterdrops against targets of annealed electrolytic tough pitch copper is shown in figure 13 along with experimental points obtained elsewhere.[2] The targets were prepared at the NBS. The static yield strength (0.2% offset) of the metal used was determined by Irwin; the average value was 3,975 psi. The dynamic compressive yield strength used for E' in eq (21) was that given by Whiffin (table 2) for electrolytic copper. The speed of sound in infinite medium determined for electrolytic tough pitch copper by Tschiegg (table 2) was used for c' and in computing z'. There is quite a bit of scatter in the data plotted in figure 13. However, both the slope and intercept of the calculated line are in relatively good agreement with these data.

The pit-depth-versus-velocity curve calculated by use of eqs (21) and (22) for collisions of 0.2-cm waterdrops against targets of 2024–0 aluminum is

shown in figure 14 with experimental points obtained elsewhere.[2] The targets were prepared at the NBS. They were made of the same 2024 aluminum as the targets that were used for collisions with mercury drops (see sec. 2.6b and fig. 12), and the same values of E', c', and z' were used in calculating the pit-depth-versus-velocity curve. It can be seen from figure 14 that the calculated line fits the experimental points fairly well.

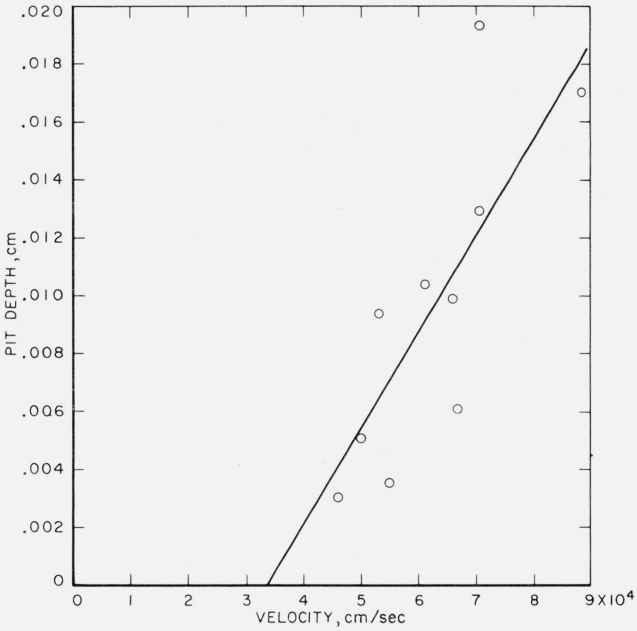

FIGURE 13. *Calculated curve for collisions of 0.20-cm waterdrops against target plates of electrolytic tough pitch copper.*

⊙ observed depth for 0.20-cm drop.

The pit-depth-versus-velocity curve calculated by use of eqs (21) and (22) for collisions of 0.2-cm waterdrops against lead targets is shown in figure 15. The experimental points shown in the graph were obtained elsewhere.[2] The kind of lead that was used for the targets is not known. The dynamic yield strength used for E' was that given by Whiffin (table 2) for 99.97 percent pure lead. The speed of sound in infinite medium for pig lead determined by Tschiegg was used for c' and in computing z'.

The amount of agreement that has been found between the calculated curves and experimental points for collisions of both mercury drops and waterdrops with targets of copper, 2024–0 aluminum, and lead may be favorable evidence for the possible usefulness of eq (22) in predicting corresponding velocities-for-equal-pit-depth for collisions of metal target plates with waterdrops and with mercury drops.

2.7. Corresponding Velocities-for-Equal-Pit-Depth

From the standpoint of the problem of high-speed rain erosion, the practical value of an equation giving the depth of damage pits as a function of impingement velocity is its use to extrapolate from the

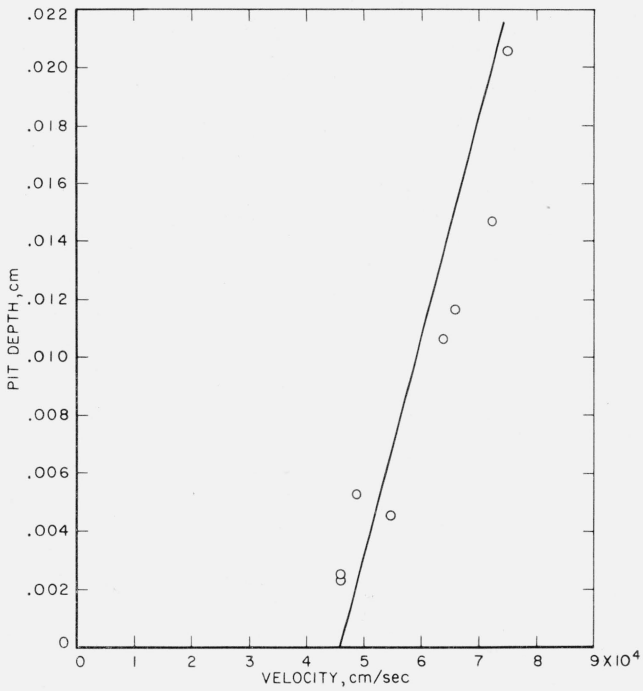

FIGURE 14. *Calculated curve for collisions of 0.20-cm waterdrops against target plates of 2024–0 aluminum.*

⊙ observed depth for 0.20-cm drop.

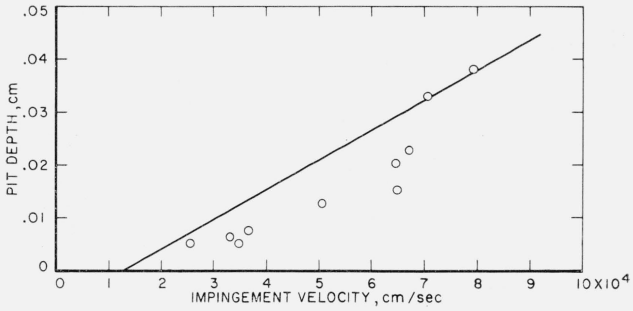

FIGURE 15. *Calculated curve for collisions of 0.20-cm waterdrops against target plates of lead.*

⊙ observed depth for 0.20-cm drop.

known depth of pit produced by collision of a solid target with a drop of high-density liquid at a relatively low impingement velocity to the depth of pit that would be produced on the same target material by collision with a drop of low-density liquid, such as water, at a very much higher impingement velocity. The purpose of carrying out this extrapolation is to bypass the necessity of firing target materials at the extremely high velocities for which test results are desired for collisions of solids with waterdrops.

If drops of a liquid A having diameter d_A collide with a solid material having acoustic impedance z' and dynamic yield strength E', eq (22) predicts that the pit depth will be

$$\delta_A' = \frac{7.2 d_A z_A}{c_A(z_A + z')}[V_A - V_{iA}], \tag{23}$$

where V_{iA} is the intercept velocity calculated with use of eq (21) and with use of the density and acoustic impedance of liquid A for ρ and z, respectively. The depth of pits resulting from collisions of drops of liquid B with the same solid material will be

$$\delta_B' = \frac{7.2 d_B z_B}{c_B(z_B + z')}[V_B - V_{iB}], \tag{24}$$

where V_{iB} is the intercept velocity calculated with use of eq (21) and with use of the density and acoustic impedance of liquid B for ρ and z, respectively.

If the depth of pits produced by collision of the solid target with drops of liquid A is to be the same as that produced by collision of the solid target with drops of liquid B, then, by equating δ_A' and δ_B' given by eqs (23) and (24),

$$V_A = \frac{d_B z_B c_A (z_A + z')}{d_A z_A c_B (z_B + z')} V_B - \frac{d_B z_B c_A (z_A + z')}{d_A z_A c_B (z_B + z')}\left[\frac{19 E'(z_B + z')}{(\rho_B c' z'^3)^{1/2}}\right] + \frac{19 E'(z_A + z')}{(\rho_A c' z'^3)^{1/2}}. \tag{25}$$

All quantities are expressed in cgs units. The dynamic compressive yield strength must be used for E' and the sound speed in infinite medium must be used for c' and in computing z' in making calculations with this equation.

2.8. Applicability of the Damage Equation

It was remarked in section 2.2 that the extent and type of damage produced on solids as a result of collision with liquid drops depends strongly on the characteristic properties of the solid, and that if the damage is to be described by an equation, it will be necessary to develop separate equations for the damage produced on solid materials that have widely different properties. It was pointed out that the simplest case to consider is that of materials such as the soft and medium hard metals that undergo permanent plastic flow without fracture as a result of collision with liquid drops. Equation (22) has been developed to describe the depth of pits that will be produced in materials of this kind as a result of such collisions. It cannot validly be applied beyond the limits of the model on which it was constructed.

Equation (22) is restricted to damage associated with the impact pressure that results when a solid target collides with a liquid drop at high speed. The dimensionless Reynolds number, Weber number, and surface tension quotient, which are associated with the radial flow of the drop, were deleted from eq (7) to produce eq (8), and eq (22) contains only the dimensionless quotients that appear in eq (8). In view of this restriction on eq (22) it can be expected that there will be limits on its application even to the soft and medium hard metals.

In discussing the agreement of the calculated curve with the experimental points for lead target plates it was pointed out that for metals as soft as lead at very high collision velocities the radial flow of a mercury drop drags metal up the walls of the damage pit and piles it up at the mouth of the crater. This mode of forming, or of deepening, a pit was not considered in the development of eq (22), and eq (22) will not adequately describe pits that were produced either wholly or appreciably by this mechanism. It is noteworthy that where this additional pit-forming mechanism does not operate (in the low-velocity range), eq (22) does adequately describe the pits that are formed in lead.

Two other points should be mentioned with regard to the valid use of eq (22) for determining the depth of pits that will be produced in collisions between target plates of the medium hard metals (to which it applies) and liquid drops. One is the mode of mounting the plate of solid material with which the liquid drops collide; the other is the thickness of this plate. The reverse side of the plate must be maintained as a free surface for otherwise the core of solid material through the metal plate under the contact or collision area cannot move freely with respect to the remainder of the plate, which is an essential of the model on which eq (22) is based. The bulge on the reverse side of the 1100-aluminum plate shown in picture 6 of figure 2 appears to indicate that this condition was sufficiently realized in the mounting of the metal plates that were used for the mercury drop experiments.[2] If this condition is not realized, eq (22) cannot be applied to the pit depths that are obtained. The thickness of the plate should not be less than 1.5 to 2.0 times nor greater than 4 to 5 times the diameter of the impinging liquid drops. If the plate is too thin, the model on which eq (22) is based will break down because the plate will bend as a unit under the collision blow. If the plate is too thick, the spreading of the compressional wave on passing through it may cease to be negligible.

Equation (22) was constructed on the assumption of permanent plastic flow of the material of the target plate. The dimensionless quotient e'/E' of eq (7), which represents the resilience of the plate material, has been neglected. Consequently, eq (22) cannot validly be applied to determine the depth of pits that will form in highly resilient materials such as the polymers and rubbers when they collide with liquid drops. In the case of such materials the core of target material depressed as a result of the collision tends to spring back into its original position; the permanent damage mark that remains after the collision is more nearly a circular cut than a pit.

Equation (22) has been constructed using a very simple model. To determine how the Reynolds number and the Weber number should be introduced into eq (22), pit-depth-versus-velocity data should be obtained on a single metal for the condition that

the viscosity and surface tension of the drop liquid are gradually changed (such as by the use of glycerol-water solutions). To determine how the sound speed, c, of the liquid should appear in the expression for the intercept velocity, data should be obtained using the same metals that have been used already and a liquid that has a sound speed different from those of water and mercury, which are nearly the same. Chloroform has a sound speed about 68 percent that of water. The sound speed of water can be increased by adding sodium chloride. The speed of sound in a 20 percent sodium chloride solution is about 13 percent greater than that in fresh water and it is indicated that increase in the salt concentration will further increase the sound speed.

Finally, more pit-depth-versus-velocity data should be obtained for collision of both mercury drops and waterdrops against target metals whose dynamic compressive yield strengths are known. Whiffin [7] has determined the dynamic compressive yield strength of standard silver (7.5% Cu, 92.5% Ag), electrolytic copper, 99.97 percent lead ,and Armco iron (0.016% C, 0.006% Si, 0.017% S, 0.003% P, and 0.030% Mn). In the process of verifying eq (22) it is important to use target materials whose dynamic compressive yield strengths are known, and the same target material should be used throughout where drops of different liquids are used. If eq (22) is fully verified, it can be used to determine the dynamic compressive yield strength of other metals.

3. Collisions Between Metal Plates and Flowing Metal Spheres

Partridge, VanFleet, and Whited [11] fired spheres of zinc, tin, copper, lead, aluminum, and iron against targets of the same material at collision velocities up to 24×10^4 cm/sec (7,900 ft/sec) and maintained conditions such that the spherical pellet lost no mass before striking the target. They found that the penetration varied linearly with velocity for the materials used and the velocity range investigated. They reported that the pellets flowed during the collisions.

In the light of the fact that the pellets flowed during the collisions, it is reasonable to suppose that the pit-depth-versus-velocity equation that was developed for collisions of metal targets with liquid drops, eqs (21) and (22), should apply to this case without modification. When the material of the target is the same as the material of the projectile, eqs (21) and (22) simplify to

$$\delta'=3.6\ d\ (V-V_i)/c \tag{26}$$

and

$$V_i=38\ E'/z \tag{27}$$

Some of the pit-depth-versus-velocity data [11] are plotted in figures 16, 17, 18, 19, and 20 along with curves calculated by use of eqs (26) and (27). The physical properties of the metals used by Partridge et al. [11] were not determined. The physical constants used for these materials in eqs (26) and (27) are given in table 2.

3.1. Collisions of Iron Spheres Against Iron Targets

It is assumed that soft, relatively pure iron was used in these experiments [11] because the spherical pellets fired were made by placing fragments of the metal in the hemispherical cavities of a case-hardened steel tool and pressing the two sections together. The diameter of the pellets for which the experimental pit-depth-versus-velocity data are given in figure 16 was 0.483 cm. The calculated curve is shown in figure 16 along with the experimental points which are indicated with circles. The observed pit depths for iron spheres colliding with iron targets are in good agreement with the calculated curve up to a collision velocity of 24×10^4 cm/sec (7,900 ft/sec). This velocity is, however, less than half the speed of sound in infinite medium for iron (58.5×10^4 cm/sec).

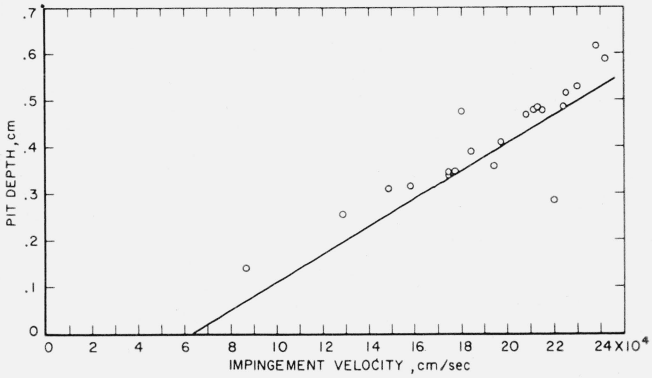

FIGURE 16. *Calculated curve for collisions of 0.483-cm iron spheres against iron targets.*

⊙ observed depth for 0.483-cm sphere.

3.2. Collisions of Aluminum Spheres With Aluminum Targets

Values for physical constants of 1100–0 aluminum were used in eqs (26) and (27). The value of the dynamic compressive yield strength used for E' in eq (27) was computed from a ratio of the dynamic to the static yield strength of 4; this is a rough ratio estimated by Whiffin [10] for an 1100–0 aluminum having an average static yield strength of 2,625 psi.

Very few experimental pit depths were given by Partridge et al. [11] for collisions of 0.483-cm aluminum spheres with aluminum targets. The data available contain quite a bit of scatter. They are plotted in figure 17 along with the curve calculated using eqs (26) and (27). There is reasonably good agreement with the calculated curve. The highest collision velocity for which a pit depth was reported is approximately one-third of the speed of sound in aluminum.

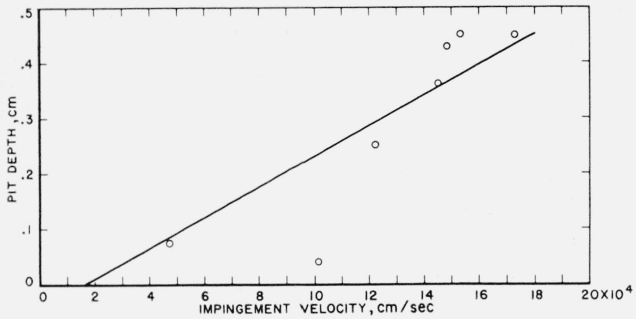

FIGURE 17. *Calculated curve for collisions of 0.483-cm aluminum spheres against aluminum targets.*

⊙ observed depth for 0.483-cm sphere.

3.3. Collisions of Lead Spheres Against Lead Targets

Whiffin [7] determined the dynamic compressive yield strength of lead that was 99.97 per cent pure and this value of the dynamic compressive yield strength was used for E' in eq (27). The sound speed in infinite medium was determined by Tschiegg (table 2) both for chemical lead and for pig lead. The theoretical curve computed using the sound speed for pig lead is shown in figure 18 along with the pit-depth-versus-velocity data obtained by Partridge et al. [15] for 0.483-cm lead spheres impinging against lead targets.

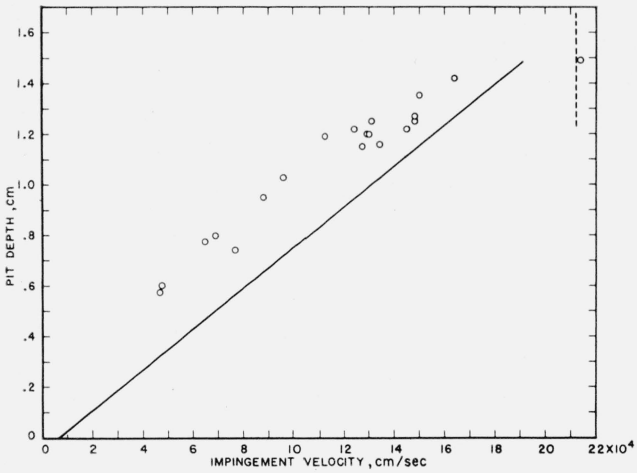

FIGURE 18. *Calculated curve for collisions of 3/16-in. lead spheres against lead targets.*

⊙ observed depth for 3/16-in. sphere.

The experimental pit depths found at the high velocities used are all greater than eq (26) would predict. No data were obtained in the low velocity range where the calculated curve was found to fit the data for collisions of lead target plates with mercury drops. See section 2.6a, where the possibility that two mechanisms contribute to the formation of pits in lead at high collision velocities is discussed.

The speed of sound in infinite medium for pig lead is marked with a vertical dotted line in figure 18. It would appear from the empirical data at the highest velocities used that the experimental pit-depth-versus-velocity curve for lead is flattening at velocities above the speed of sound in lead.

It appears from the data that have been presented in the preceding sections that, at collision velocities for which an originally solid target remains solid during the collision, pit depth is a straight-line function of collision velocity if the rear face of the target plate is a free surface. This appears to be the case regardless of whether the projectile was originally solid and remains solid during the collision (low-speed solid-to-solid collisions), whether the projectile was originally solid but flows during or as a result of the collision (high-speed solid-to-solid collisions), or whether the projectile was originally a liquid drop (liquid-to-solid collisions). At extremely high (meteoric) collision velocities it appears that an originally solid target may be expected to behave like a liquid during the collision because of the enormous impact pressure developed. With regard to collisions of this kind Öpik [13] has stated that the aerodynamic ($1/2\ \rho V^2$) pressure at the penetration of a meteor into rock is more than 1,000 times the plastic limit of steel; he has hypothesized that all solid materials under such pressures must behave like liquids and that the problem of meteor impact is the case of the impact of a liquid drop of one density into a liquid medium of a different density. Under such conditions the penetration or pit depth may become independent of the collision velocity, or may become essentially so, and the pit-depth-versus-velocity curve may approach a horizontal line parallel to the velocity axis. A trend in this direction may be indicated by the flattening of the experimental pit-depth-versus-velocity curve for lead. Whenever this condition is realized, either partially or completely, the pit-depth-versus-velocity equation developed in this paper will no longer be applicable.

3.4. Collision of Copper Spheres Against Copper Targets

The data for impingement of 0.483-cm copper spheres against copper targets [11] are shown in figure 19 along with the theoretical curve calculated by eqs (26) and (27) using physical constants for electrolytic copper (table 2).

The empirical pit-depth-versus-velocity curve for copper appears as though it may be flattening at the highest collision velocities for which data were obtained, as was found in the case of lead. If this is indeed true, it raises the question as to what determines the flattening of the curve. In the case of lead it happened at collision velocities equal to the speed of sound in lead. If it is happening for copper at velocities of 16×10^4 to 18×10^4 cm/sec, it is happening at velocities that are about half the speed of sound in copper. The speed of sound in infinite medium for electrolytic tough pitch copper is 46.91 $\times10^4$ cm/sec. It does not, furthermore, seem to be

related to the melting point of the target material because copper has a high melting point and lead has a very low one. A possible explanation is the relative susceptibility of the target material to flow by translational slip of the target atoms on their lattice planes at high rates of loading. With regard to the use of copper as a liner for shaped charges, Rinehart and Pearson [14] state that copper flows readily at high rates of loading.

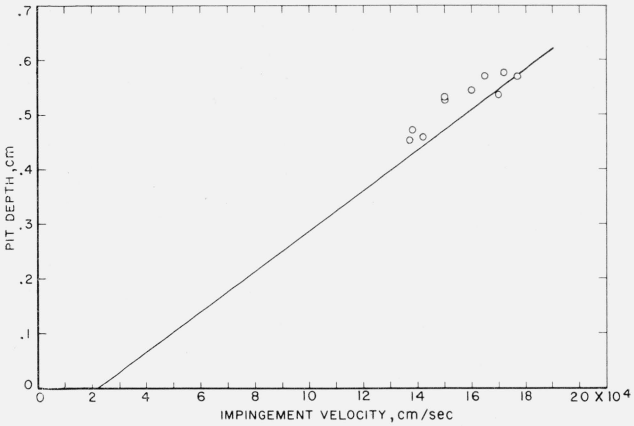

FIGURE 19. *Calculated curve for collisions of 0.483-cm copper spheres against copper targets.*

⊙ observed depth for 0.483-cm sphere.

3.5. Collisions of Zinc Spheres Against Zinc Targets

No value of the dynamic compressive yield strength of zinc was obtainable. One of the possible uses of the pit-depth-versus-velocity equation reported in this paper is the calculation of the dynamic compressive yield strength from pit-depth-versus-velocity data. By trial it was found that to obtain an acceptable value of the intercept velocity for zinc with the pit-depth-versus-velocity data of Partridge et al. [11], the value of the dynamic compressive yield strength for zinc would be 1.546×10^9 d/cm^2. The experimental pit-depth-versus-velocity data for zinc and the line calculated from eqs (26) and (27) using this value of the dynamic compressive yield strength and the physical constants given in table 2 are shown in figure 20. The agreement between the experimental points and the theoretical curve is reasonably good. The two points obtained at the highest velocities used seem to show a flattening of the curve. More experimental data are needed to determine whether this is the case.

WASHINGTON, January 29, 1959.

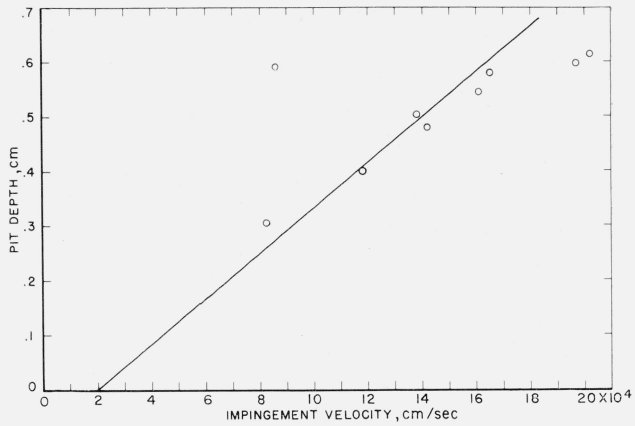

FIGURE 20. *Calculated curve for collisions of 0.483-cm zinc spheres against zinc targets.*

⊙ observed depth for 0.483-cm sphere.

3.6. Collisions of Tin Spheres Against Tin Targets

Partridge et al. [11] also obtained pit-depth-versus-velocity data for collisions of tin spheres against tin targets. The tin appeared to crack and break off rather than to flow plastically around the crater. This interesting fact recalls the similarity in behavior of materials at low temperature and at high rates of loading. At low temperature tin tends to exist in the brittle gray tin form. It is doubtful whether the pit-depth-versus-velocity equation can be validly applied to tin because of the energy that is diverted from pit formation into crack formation (see section 2.8).

4. References

[1] Olive Engel, NBS J. Research **61,** 47 (1958).
[2] Olive Engel, NBS J. Research **54,** 281 (1955).
[3] E. Buckingham, Phys. Rev. **4,** 345 (1914).
[4] E. Buckingham, Phil. Mag. **42,** 696 (1921).
[5] P. W. Bridgman, Dimensional Analysis (Yale University Press, 1931).
[6] Garrett Birkhoff, Hydrodynamics (Princeton University Press, 1950).
[7] A. C. Whiffin, Proc. Roy. Soc. [A] **194,** 300 (1948).
[8] Communicated by letter.
[9] J. M. Krafft and A. M. Sullivan, Trans. Am. Soc. Metals **51,** (1957) (Preprint).
[10] Communicated by letter.
[11] William S. Partridge, Howard B. VanFleet, and Charles R. Whited, J. Appl. Phys. **29,** 1332 (1958).
[12] L. Bergmann, Der Ultraschall, S. Hirzel, Stuttgart (1954).
[13] Ernst Öpik, Researches on the physical theory of meteor phenomena I, Toimetused, Acta et Commentationes (Universitatis Tartuensis XXX [A] **4,** (1936, Tartu, Estonia).
[14] John S. Rinehart and John Pearson, Behavior of metals under impulsive loads, Am. Soc. Metals (1954).
[15] Howard B. VanFleet, Charles R. Whited, and William S. Partridge, High velocity impact craters in lead-tin alloys, Tech. Rpt. No. OSR–13, Dept. of Elec. Eng., University of Utah, Salt Lake City, Utah (Jan. 1958).